THE MATHEMATICAL PHYSICS OF MARINE PARTICLE AGGREGATION: A COMPUTATIONAL EXPLORATION OF THE SMOLUCHOWSKI COAGULATION EQUATION

By

TRIVIK SHAILENDRA RAGHA

A thesis submitted to the

School of Graduate Studies

Rutgers, The State University of New Jersey

In partial fulfillment of the requirements

For the degree of

Master of Science

Graduate Program in Oceanography

Written under the direction of

Kay D. Bidle

And approved by

_____

_____

_____

_____

New Brunswick, New Jersey

October 2024

ABSTRACT OF THE THESIS

The Mathematical Physics of Marine Particle Aggregation:

A Computational Exploration of The Smoluchowski Coagulation Equation

By TRIVIK SHAILENDRA RAGHA

Thesis Director

Dr. Kay D. Bidle

Marine particle aggregation plays a crucial role in the global carbon cycle by transporting and sequestering carbon from the surface ocean to the deep sea. This thesis explores the mathematical physics of marine particle aggregation using the Smoluchowski Coagulation Equation (SCE). The primary goal is to evaluate the continuous deterministic version of the SCE and derive insights to enhance future modeling efforts of how particles form. Traditional methods for solving the SCE, such as The Method of Moments, the Sectional Approach, and the Fixed Pivot Method, offer various advantages in certain contexts but require a thorough understanding of the mathematics of the SCE. This study employs a direct algorithm for solving the SCE, leveraging Python's SciPy.Integrate module to calculate gains and losses of particle concentrations and SciPy.solve_ivp to solve the time derivative of mass-concentrations. The direct algorithm provides a transparent

means to explore the fundamental dynamics described by the SCE. This approach is valuable for introductory and exploratory modeling efforts. The numerical model uses an array of primary particle diameters to generate 50 discreet masses, simulating the aggregation dynamics over time, while incorporating critical microscale physical components driving encounters. Marine aggregates, which are influenced by convergence of phytoplankton physiology, microscale physics, and aggregation dynamics, are integral to the biological ocean pump. These aggregates form from encounters of primary particles (cells) through complex interactions involving fluid shear, differential settling, and Brownian motion, which are quantified by rectilinear and curvilinear coagulation kernels. Rectilinear kernels often overestimate collision frequencies by ignoring hydrodynamic effects, while curvilinear kernels provide more accurate predictions by accounting for these effects. Hence simulations with rectilinear kernels show that aggregation happens more rapidly than with simulations using curvilinear kernels.

Results indicate that particles within the 400-500 μm size range exhibit a net positive gain in mass concentration, whereas particles smaller than 400 μm experience a net loss. The phenomenon of "gelation," where particle mass aggregates into a single large cluster, was observed, leading to a decrease in total observed mass. This effect underscores the need for a deeper understanding of the SCE and the development of more complex modeling approaches to accurately capture the dynamics of particle aggregation.

Table of Contents

I. Introduction

This thesis integrates the microscale physics of marine particle aggregation with the Smoluchowski Coagulation Equation to study an essential component of the biological carbon pump - the dynamics of particle formation - from a mathematical perspective using a numerical model. The primary goal is to evaluate the suitability of the continuous deterministic version of the Smoluchowski Coagulation Equation and to derive insights that can inform and enhance future modeling efforts.

i. Phytoplankton Physiology and Microscale Physics

Marine particle aggregation is a fundamental and complex process in the ocean, which is integral to the biological carbon pump and global carbon cycle. In the euphotic zone, primary producers like phytoplankton fix atmospheric carbon dioxide into their cells via photosynthesis, initiating the biological carbon pump by removing carbon from the atmosphere and into particulate matter in the surface ocean (Guidi et al., 2016). A key area of investigation in oceanography is the subsequent processes that determine marine particle formation and the subsequent efficiency of transport of carbon from the surface to the deep ocean. The Marine Curve (Martin et al., 1987) is a common construct that describes the relationship between organic carbon flux and depth (via sinking), and provides a way to quantify the amount of carbon transport to the deep sea. Central to this curve is the B-term (detailed in the Appendices), or attenuation coefficient, which is crucial as it determines the rate at which carbon flux decreases with depth. The complexities of phytoplankton physiology, microscale physics, and aggregation dynamics significantly influence the B-term. For instance, viral infection of phytoplankton during a bloom leads to a dramatic increase in transparent exopolymer particles (TEP), which enhances particle "stickiness" and leads

to greater marine particle aggregation (Engel, 2000). This process has been observed to for both diatoms (Yamada et al., 2018) and coccolithophores (Laber et al., 2018) populations. In this case, the overarching effect of an infection on a population of phytoplankton is to enhance particle aggregation and shuttle particulate organic matter (POM) to the deep ocean (Locke et al., 2022), effectively lowering the B-term and promoting carbon flux to greater depths. Depending on the phytoplankton composition, the nature of host-virus interactions and prevailing sea states (microscale physics), viruses can also lyse phytoplankton and stimulate upper ocean remineralization and respiration of dissolved organic matter (DOM), thereby increasing the B-term and preventing carbon sequestration (Locke et al., 2022). This complex interplay between phytoplankton physiology, marine viruses, and microscale physics, which fundamentally determines if marine particles form and aggregate, ultimately impacts the flux of the carbon to the deep sea and is a critical part of the biological carbon pump. The controls on aggregation of POM into marine snow particles under different physical regimes is the focus of this thesis.

Phytoplankton particles (cells) can encounter and coagulate with each other and with other marine particles in the water column forming marine aggregates (Burd & Jackson, 2009). The rates at which particles encounter each other are called encounter rates, and microscale interactions that lead to aggregation are primed by encounters between marine particles (Słomka et al., 2023). Encounters are affected by the behavior of particles in fluid flow such as fluid shear due to laminar and turbulent flow regimes, differential settling due to sinking, Brownian motion due to random collisions, as well as the concentrations of particles in the medium.

The continuous and deterministic Smoluchowski Coagulation Equation (SCE) models particle aggregation. This integro-differential equation is based on the premise that two particles of size r and s can combine to form an aggregate of size $r + s$, expressed as $C_r + C_s \rightarrow C_{r+s}$ (Wattis,

2006). Since mass is additive, the resulting aggregate mass is the sum of the individual particle masses. The SCE is given in equation (1) below:

$$\frac{dC(m,t)}{dt} = \frac{\alpha}{2}\int_0^m \beta(m_j, m-m_j)C(m-m_j,t)C(m_j,t)dm_j - \alpha C(m,t)\int_0^\infty \beta(m,m_j)C(m_j,t)dm_j. \quad (1)$$

Equation (1) balances the time rate of change of particle concentrations of size m, denoted by $C(m,t)$, by considering both the gain from the aggregation of smaller particles and the loss from their coalescence with other particles. The encounter rates are incorporated into coagulation kernels, β, and the particle stickiness is incorporated into the equation by the parameter α. Modeling aggregation dynamics under different condition states using the SCE can enhance our understanding of the biological carbon pump by allowing us to better predict the controls on aggregate formation and to improve future carbon flux models.

II. Methodology

The numerical model designed for this thesis solves the SCE in a direct manner. While there are various methods to solve the SCE, such as The Method of Moments (TMOM) (Islam et al., 2023), the Sectional Approach (Jackson, 1990), and the Fixed Pivot Method (Kumar & Ramkrishna, 1996), the present model employs a direct algorithm for simplicity and direct application of the equation. This approach is valuable for introductory and exploratory modeling efforts, providing a foundation for further refinement and comparison with more complex methods. The model calculates 50 discreet masses, from a user provided array of particle diameters, to solve the gains and losses terms in equation (1) using Python's SciPy. Integrate module. The time derivative of the

mass-concentrations function is solved via Python's SciPy.solve_ivp module given an initial set of number concentrations for those 50 discreet mass points at time $t = 0$ seconds.

i. Aggregate Cluster Size Calculation

To simplify the numerical modelling, all marine particles were of the same composition and had perfect spherical form with uniform mass-to-volume density. In reality, marine particles and aggregates are often non-spherical, have a certain degree of porosity and can vary in composition and density (e.g., due to the presence of biominerals and/or mucous). The simplification allows us to first test fundamental principles of aggregation before layering particle complexities. It is possible to map the mass of a particle/aggregate to its equivalent radius by means of a fractal dimension, which gives a measure of how the particles scale in the spatial dimension with respect to mass (Li & Logan, 2001). In general, this mass-radius relationship is as follows, $m \propto r^{D_f}$. For spherical particles with uniform density, the fractal dimension, D_f, is equal to 3. Hence $m \propto r^3$. Using the standard equations of density and volume of a sphere, the equation that maps the particles mass, m, to its radius, r, based on its density, ρ_p, is given by:

$$m = \rho_p \times \frac{4}{3} \times \pi \times r^3. \quad (2)$$

This model also assumes that the aggregate structure is scale-invariant, meaning that the fractal dimension remains constant regardless of the aggregate size. However, when the structure of aggregates is not scale-invariant, determining the fractal dimension using the mass-radius relationship can produce inaccuracies, leading to overestimated values (Gmachowski, 2002). The standard units used in the model for mass, density, and radius are grams, grams per cubic centimeter, and centimeters, respectively.

ii. Aggregate Sinking Velocity Calculations

A significant advantage of assuming spherical aggregates with uniform density allows for the calculation of aggregate settling velocities using the Stokes regime. This assumption simplifies the calculations and enables the application of Stokes' Law, which is suitable for small, smooth, and rigid spheres settling at low Reynolds numbers (Laurenceau-Cornec et al., 2019). Stokes' Law provides a straightforward method to estimate the sinking velocity, *W*, from particle density, ρ_p, fluid density, ρ_f, gravitational acceleration, a_g, dynamic viscosity, μ, and radius, *r*, using the equation:

$$W = \frac{2}{9} a_g \left(\frac{\rho_p - \rho_f}{\mu} \right) r^2. \quad (3)$$

It is important to recognize that the application of Stokes' Law to marine aggregates is an approximation. Marine aggregates are complex in shape, structure, and composition, which can significantly alter their sinking behavior. For instance, non-spherical particles experience different drag forces compared to spherical ones, and their sedimentation behavior can be described using more complex models, such as the Navier-Stokes drag equation, which accounts for shape and surface roughness (Dogonchi et al., 2015). Furthermore, the sinking dynamics of marine aggregates are influenced by the balance between biomineral ballast, which increases sinking speed, and mucus coatings, which slow it down, affecting their overall descent through the water column and residence time in the upper ocean (Chajwa et al., 2023).

iii. Defining The Coagulation Kinetic (Encounter) Rate Functions

Coagulation Kernel	Rectilinear Form	Curvilinear Form
Brownian Motion $\boldsymbol{\beta_{br}(r_i, r_j)}$	$\frac{K_B T_K}{\mu}\frac{(r_i + r_j)^2}{r_i r_j}$	None
Laminar Shear $\boldsymbol{\beta_{ls}(r_i, r_j)}$	$\frac{4}{3}\gamma(r_i + r_j)^3$	None
Turbulent Shear $\boldsymbol{\beta_{ts}(r_i, r_j)}$	$1.3\left(\frac{\epsilon}{\nu}\right)^{\frac{1}{2}}(r_i + r_j)^3$	$9.8\frac{p^2}{1+2p^2}\left(\frac{\epsilon}{\nu}\right)^{\frac{1}{2}}(r_i + r_j)^3$ $p = \frac{\min\{r_i, r_j\}}{\max\{r_i, r_j\}}$
Differential Sedimentation $\boldsymbol{\beta_{ds}(r_i, r_j)}$	$\pi(r_i + r_j)^2\lvert w_i - w_j\rvert$	$\frac{1}{2}\pi(r_i)^2\lvert w_i - w_j\rvert$

Table 1. Radius input forms for each coagulation kernel. The variables r_i and r_j are the radii of particle *i* and *j* respectively. The parameters $K_B, T_K, \mu, \gamma, \epsilon$, and ν are the Boltzmann Constant, thermodynamic temperature, kinetic viscosity, shear gradient, kinetic energy dissipation rate, and dynamic viscosity respectively.

Equations (2) and (3) can be used to convert the coagulation kernels in Table 1.1 (Burd & Jackson, 2009) from radius input form, $\beta(r_i, r_j)$, to mass input form $\beta(m_i, m_j)$. The mass input forms for the coagulation kernels are more compatible with Equation (1). These kernels quantify the encounter rates of marine particles and serve as a first order pre-requisite for aggregation. Rectilinear kernels often overestimate collision frequencies by ignoring hydrodynamic effects, whereas curvilinear kernels account for these effects and provide more accurate predictions (Burd & Jackson, 2009). For the simulations, a turbulent flow regime is assumed. The sum of all rectilinear kernels (excluding the Laminar Shear kernel) is used for rectilinear simulations, while curvilinear simulations use the rectilinear kernel for Brownian Motion and curvilinear kernels for

Turbulent Shear and Differential Sedimentation. Both rectilinear and curvilinear simulations are conducted for comparative purposes.

iv. Defining The Initial Number Concentrations Functions

The distribution of the concentrations of a particular cluster size is known as a Particle Size Distribution (PSD). Naturally occurring PSDs in the ocean can be measured by laser diffraction techniques. One instrument that does this is the Laser In-Situ Scattering and Transmissometry (LISST) instrument manufactured by Sequoia Scientific. Whilst the LISST instrument provides realistic PSDs for initial and final particle populations to quantify aggregation and derive stickiness (Engel, 2000), it is first useful and necessary to study the results of initializing the SCE with PSDs of known functional forms to better understand the mathematics involved in using the SCE for aggregation modelling. This provides opportunities to improve upon the numerical model and allow for naturally occurring PSDs (as measured by the LISST) to be initialized into the model for simulation under different condition states.

Four different initial conditions were investigated using the numerical model: a constant distribution, a linear distribution, a normal distribution, and a trigonometric distribution, each with exact mathematical representations at time $t = 0$. The initial conditions consist of 50 discreet mass points ranging from 1 to 500 micrometers. The constant distribution sets a uniform concentration of 5000 particles. The linear distribution varies from 0 to 5000 particles. The normal distribution, centered at 100 micrometers with a standard deviation of 100 micrometers, is scaled by a factor of 100. The trigonometric distribution uses sine functions to create a periodic pattern, scaled to approximately 3000 particles.

III. Results

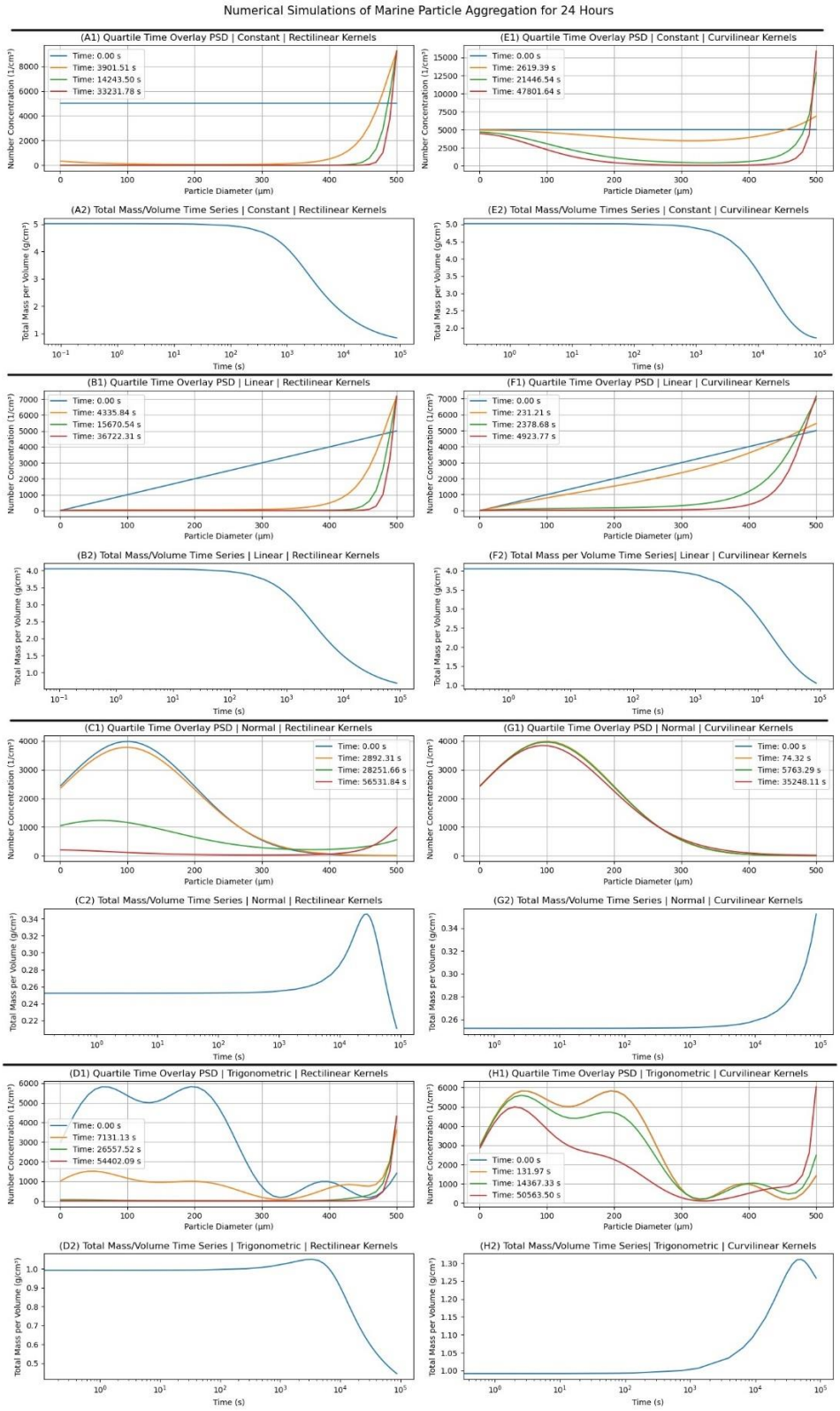

Figure 1. Simulation results for rectilinear (Plots A-D, left column) and curvilinear (Plots E-H, right column) forms of coagulation kernels for all defined functional initial mass concentrations. The corresponding mass per volume plot lies underneath the Overlay PSD for each simulation.

Figure 1 above shows the results of simulating marine particle aggregation over 24 hours for particles ranging from 1 μm to 500 μm. Simulating aggregation for both rectilinear and curvilinear kernels provide a comparative and exploratory analysis of particle interactions, conducted as an academic exercise to understand the nuances of the mathematics of the SCE. As expected, simulations using the curvilinear kernels exhibit slower time evolutions of the PSD compared to the simulations involving the rectilinear kernels. However, the simulations involving both rectilinear and curvilinear kernels exhibit similar trends. Particles in the 400 μm to 500 μm ranges experience a net positive gain in mass concentrations, while particles smaller than 400 μm experience a net loss in mass concentrations during the time span of the simulation. All simulations tend to experience an overall decrease of total mass per volume. The simulations with constant and linear initial mass concentration distributions remain relatively steady before rapidly decreasing, whilst the simulations with the normally distributed and trigonometric initial mass concentrations remain relatively steady, then increase and then rapidly decrease with time. Note that the mass per volume plot for the Normally distributed initial mass concentration only shows a rapid increase in mass concentration after remaining relatively constant. It can be assumed with high confidence that total mass per volume will decrease rapidly, given a longer simulation time following the trend of the corresponding mass per volume plot for the rectilinear simulation. Simulations Plots for both rectilinear and curvilinear kernels can also be found in the Appendices.

IV. Discussion and Conclusion

Upon inspection of equation (1), if the gains in mass concentration for a particular size cluster exceed the losses at a particular time step, the time rate of change of the number concentration is positive, resulting in an increase in mass concentration for that particle size. Likewise, if the losses in mass concentration for a particular size cluster exceed the gains at a particular time step, the

time rate of change of the number concentration is negative, resulting in a decrease in mass concentration for that particular size. The former seems to be the case for particles of cluster sizes between 400 μm and 500 μm, whilst the latter seems to be the case for particle cluster sizes less than 400 μm throughout each simulation. Additionally, the total mass of the system is not conserved for each simulation. This phenomenon, known as "gelation" (Wattis, 2006) occurs when a significant fraction of the mass aggregates into a single, large cluster, often referred to as a "gel". In the context of aggregation modeling in this thesis, it is unclear whether the breakdown of mass conservation is meaningful in describing the physical phenomena of aggregation or if it results from inadequacies in modeling aggregation using the SCE. What is clear from Equation (1) is that there are more ways for a particle of a particular size to lose mass concentration due to aggregation with all other particles than there are for the particle to gain mass concentration from only smaller particles. This is true regardless of the initial distribution of mass concentration across all sizes. The model shows this behavior, especially for the initially normally distributed and trigonometric PSDs, which have a relatively high mass concentration towards the smaller sizes of primary particles. By this logic, larger particles are more likely to lose mass concentration to particles outside their size range of the model, which may explain the breakdown of mass conservation. However, it is worth noting that mass conservation and gelation are consequences of the types of kernels used in the SCE and also depend on the boundedness of the systems moments (Islam et al., 2023). Delving deeper into the mathematics of the SCE is crucial for understanding the gelation phenomena. Furthermore, the SCE may need to be looked at from a Stochastic viewpoint and may need coupling with other equations such as Reynolds Transport Theorem for more accurate modelling because a deterministic version (Equation 1) may not adequately capture the full dynamics of marine particle aggregation.

References

Burd, A. B., & Jackson, G. A. (2009). Particle aggregation. *Ann Rev Mar Sci*, *1*, 65-90. https://doi.org/10.1146/annurev.marine.010908.163904

Chajwa, R., Flaum, E., Bidle, K. D., Van Mooy, B., & Prakash, M. (2023). Hidden Comet-Tails of Marine Snow Impede Ocean-based Carbon Sequestration. *arXiv preprint arXiv:2310.01982*.

Dogonchi, A. S., Hatami, M., Hosseinzadeh, K., & Domairry, G. (2015). Non-spherical particles sedimentation in an incompressible Newtonian medium by Padé approximation. *Powder Technology*, *278*, 248-256. https://doi.org/10.1016/j.powtec.2015.03.036

Engel, A. (2000). The role of transparent exopolymer particles (TEP) in the increase in apparent particle stickiness (α) during the decline of a diatom bloom. *Journal of Plankton Research*, *22*(3), 485-497.

Gmachowski, L. (2002). Calculation of the fractal dimension of aggregates. *Colloids and Surfaces A: Physicochemical and Engineering Aspects*, *211*(2), 197-203. https://doi.org/https://doi.org/10.1016/S0927-7757(02)00278-9

Guidi, L., Chaffron, S., Bittner, L., Eveillard, D., Larhlimi, A., Roux, S., Darzi, Y., Audic, S., Berline, L., & Brum, J. R. (2016). Plankton networks driving carbon export in the oligotrophic ocean. *Nature*, *532*(7600), 465-470.

Islam, M. S., Kimura, M., & Miyata, H. (2023). Generalized Moment Method for Smoluchowski Coagulation Equation and Mass Conservation Property. *Mathematics*, *11*(12). https://doi.org/10.3390/math11122770

Jackson, G. A. (1990). A model of the formation of marine algal flocs by physical coagulation processes. *Deep Sea Research Part A. Oceanographic Research Papers*, *37*(8), 1197-1211.

Kumar, S., & Ramkrishna, D. (1996). On the solution of population balance equations by discretization—I. A fixed pivot technique. *Chemical Engineering Science*, *51*(8), 1311-1332. https://doi.org/https://doi.org/10.1016/0009-2509(96)88489-2

Laber, C. P., Hunter, J. E., Carvalho, F., Collins, J. R., Hunter, E. J., Schieler, B. M., Boss, E., More, K., Frada, M., & Thamatrakoln, K. (2018). Coccolithovirus facilitation of carbon export in the North Atlantic. *Nature microbiology*, *3*(5), 537-547.

Laurenceau-Cornec, E. C., Le Moigne, F. A. C., Gallinari, M., Moriceau, B., Toullec, J., Iversen, M. H., Engel, A., & De La Rocha, C. L. (2019). New guidelines for the application of Stokes' models to the sinking velocity of marine aggregates. *Limnology and Oceanography*, *65*(6), 1264-1285. https://doi.org/10.1002/lno.11388

Li, X.-Y., & Logan, B. E. (2001). Permeability of Fractal Aggregates. *Water Research*, *35*(14), 3373-3380. https://doi.org/https://doi.org/10.1016/S0043-1354(01)00061-6

Locke, H., Bidle, K. D., Thamatrakoln, K., Johns, C. T., Bonachela, J. A., Ferrell, B. D., & Wommack, K. E. (2022). Marine viruses and climate change: Virioplankton, the carbon cycle, and our future ocean. In *Viruses and Climate Change* (pp. 67-146). https://doi.org/10.1016/bs.aivir.2022.09.001

Martin, J. H., Knauer, G. A., Karl, D. M., & Broenkow, W. W. (1987). VERTEX: carbon cycling in the northeast Pacific. *Deep Sea Research Part A. Oceanographic Research Papers*, *34*(2), 267-285.

Słomka, J., Alcolombri, U., Carrara, F., Foffi, R., Peaudecerf, F. J., Zbinden, M., & Stocker, R. (2023). Encounter rates prime interactions between microorganisms. *Interface Focus*, *13*(2), 20220059.

Wattis, J. A. D. (2006). An introduction to mathematical models of coagulation–fragmentation processes: A discrete deterministic mean-field approach. *Physica D: Nonlinear Phenomena*, *222*(1-2), 1-20. https://doi.org/10.1016/j.physd.2006.07.024

Yamada, Y., Tomaru, Y., Fukuda, H., & Nagata, T. (2018). Aggregate Formation During the Viral Lysis of a Marine Diatom. *Frontiers in Marine Science*, *5*. https://doi.org/10.3389/fmars.2018.00167

Appendices

A1. Rationale and Design of the Numerical Model

The numerical model designed for this thesis is developed as an introductory approach to the Smoluchowski Coagulation Equation (SCE) and serves as an exploratory effort within the context of marine particle aggregation. As stated in Section 2 of Page 3, the model directly solves the SCE given by Equation (1). At its core, this means that given a user-defined range of diameters and a function that describes the initial distribution of number concentration across this diameter range, the model calculates the gains (first term on the right-hand side of Equation (1)) and losses (second term on the right-hand side of Equation (1)) for all provided diameters as the simulation advances in time. This involves numerically solving the time derivative (left-hand side of Equation (1)).

The equation solvers used in the model come from Python's scipy library, which provides powerful capabilities for solving equations. The gains and losses are calculated using scipy.integrate.quad, a function for performing numerical integration. It uses adaptive quadrature methods to evaluate definite integrals over continuous intervals, handling continuous functions and providing accurate results by adaptively adjusting the integration process based on the function's behavior. This ensures precise evaluation of these integrals by accommodating the continuous nature of the functions involved. The time rate of change of the number concentration function is handled by scipy.integrate.solve_ivp, which features adaptive time-stepping. This allows for precise temporal resolution, capturing the dynamics of particle concentrations over time with high fidelity. The combination of spatial and temporal resolution enables the model to effectively simulate the complex processes of marine particle aggregation described by the SCE.

Also mentioned in Section 2 on Page 3 of the Thesis are the other methods that researchers have used to solve the SCE. These methods are slightly more complex and involve a stronger grasp on the mathematics of the SCE. They do have some advantages though. For example, The Method of Moments (TMOM) requires some understanding of functional analysis, and knowledge of what information a k^{th} moment will produce (Islam et al., 2023) in order to accurately build an aggregation model. The advantage of this is that it simplifies the SCE by transforming it into a set of moment equations, which describe the evolution of the moments of the particle size distribution. This approach reduces complexity by eliminating the need to track the full-size distribution directly but comes at the expense of a detailed resolution because it does not solve for the distribution itself. What is also particularly notable when it comes to moments of the SCE is that there are some theorems that can be made use of in future modelling efforts for mass conservation (Islam et al., 2023).

Another method that is advantageous when it comes to mass conservation is the Fixed Pivot method. The Fixed Pivot Method (FPM) ensures mass conservation and numerical stability by discretizing the size distribution into fixed intervals and redistributing mass among these intervals during aggregation. However, developing an algorithm for this method is much more complex than the algorithm used in the model for this thesis.

The Sectional Approach involves dividing the particle size domain into sections and handling only one integral quantity (e.g., number, surface area, or volume) within each section. The integral quantity is conserved within the computational domain, and coagulations between all particle sizes are properly accounted for. Like the Fixed Pivot Method, the algorithm for this method will be a little more complex than the one used in the model for this thesis.

The numerical model used for this thesis is available on GitHub. This repository includes the full implementation of the model, source code, and detailed documentation to facilitate replication and further research. Access the repository at:

https://github.com/Triv99/Triv_MOO_Thesis24 .

A3. Table of Default Model Parameter Values

Parameter	Symbol	Default Value	Units
Boltzmann Constant	K_B	1.38×10^{-23}	J/K
Thermodynamic Temperature	T_K	293.15	K
Fluid Density	ρ_f	1.025	g/cm^3
Particle Density	ρ_p	1.200	g/cm^3
Dynamic Viscosity	μ	1.0×10^{-3}	kg/ m*s
Kinematic Viscosity	ν	$\frac{\mu}{\rho_f \times 1000}$	m^2/s
Shear Gradient	γ	1	1/s
Turbulent Energy Dissipation Rate	ϵ	1.0×10^6	m^2/s^3
Gravitational Acceleration	a_g	9.81	m/s^2

Table A1. This table lists the default values of various parameters used in the numerical model for marine particle aggregation. The parameters include physical constants, fluid properties, and model-specific variables necessary for simulating the Smoluchowski Coagulation Equation. The symbols and units for each parameter are also provided for clarity.

A4. Table of Mass Input Form for the Coagulation Kernels

To covert the coagulation kernels in Table 1 on page 5 of thesis, we first define the following constants:

$$K1 = \frac{3}{4}\frac{1}{\pi\,\rho_p},$$

$$K2 = \frac{\rho_p - \rho_f}{\mu}.$$

Then, by Equations (2) and (3), and by accounting for the physical units, the kernels in Table 1 become:

Coagulation Kernel	Rectilinear Form	Curvilinear Form
Brownian Motion $\boldsymbol{\beta_{br}(m_i, m_j)}$	$\frac{2}{3}\times 10^6 \times \frac{K_B T_{th}}{\mu}\frac{\left(m_i^{\frac{1}{3}} + m_j^{\frac{1}{3}}\right)^2}{(m_i m_j)^{\frac{1}{3}}}$	None
Laminar Shear $\boldsymbol{\beta_{ls}(m_i, m_j)}$	$\frac{4}{3}\gamma K1\left(m_i^{\frac{1}{3}} + m_j^{\frac{1}{3}}\right)^3$	None
Turbulent Shear $\boldsymbol{\beta_{ts}(m_i, m_j)}$	$1.3\left(\frac{\epsilon}{\nu}\right)^{0.5} K1\left(m_i^{\frac{1}{3}} + m_j^{\frac{1}{3}}\right)^3$	$9.8\frac{P^2}{1+2P^2}\left(\frac{\epsilon}{\nu}\right)^{0.5} K1\left(m_i^{\frac{1}{3}} + m_j^{\frac{1}{3}}\right)^3$
Differential Settling $\boldsymbol{\beta_{ds}(m_i, m_j)}$	$\frac{20}{9}\pi a_g K2K1^{\frac{4}{3}}\left(m_i^{\frac{1}{3}} + m_j^{\frac{1}{3}}\right)^2\left\lvert m_j^{\frac{2}{3}} - m_i^{\frac{2}{3}}\right\rvert$	$\frac{10}{9}\pi a_g K2K1^{\frac{4}{3}} m_i^{\frac{2}{3}}\left\lvert m_i^{\frac{2}{3}} - m_j^{\frac{2}{3}}\right\rvert$

Table A2. This table presents the coagulation kernels in their rectilinear and curvilinear forms, expressed in terms of mass inputs. These kernels are used in the numerical model to simulate marine particle aggregation, detailing the encounter rates for Brownian motion, laminar shear, turbulent shear, and differential settling.

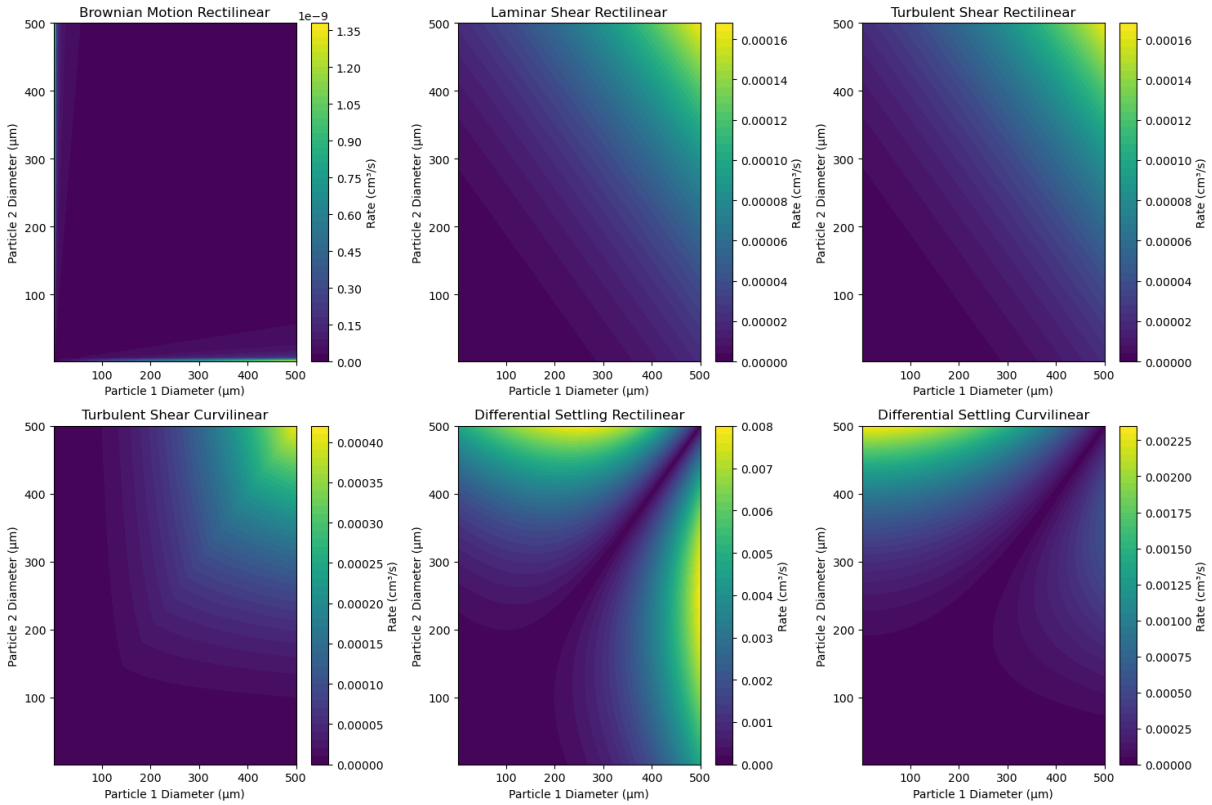

Figure A1. Coagulation Kernel Rates for Rectilinear and Curvilinear Forms. This figure displays the coagulation rates for different particle interactions based on particle diameters, shown for Brownian motion, laminar shear, turbulent shear, and differential settling. Each subplot illustrates the rate (cm³/s) as a function of the diameters of two interacting particles (Particle 1 and Particle 2). The top row presents the rectilinear forms of the kernels, while the bottom row presents the curvilinear forms, highlighting the differences in collision frequencies when hydrodynamic effects are considered.

A5. The Martin Curve Equation

The Martin Curve is mathematically expressed as:

$$F(z) = F(z_0)\left(\frac{z}{z_0}\right)^{-b},$$

where $F(z)$ is the flux of particulate organic carbon (POC) at depth z, $F(z_0)$ is the flux at a reference depth z_0, and b is the attenuation coefficient (B-term). The B-term is pivotal as it quantifies the rate at which the POC flux attenuates with depth, and thus, the efficiency of carbon sequestration in the deep ocean.

A6. Simulation Plots

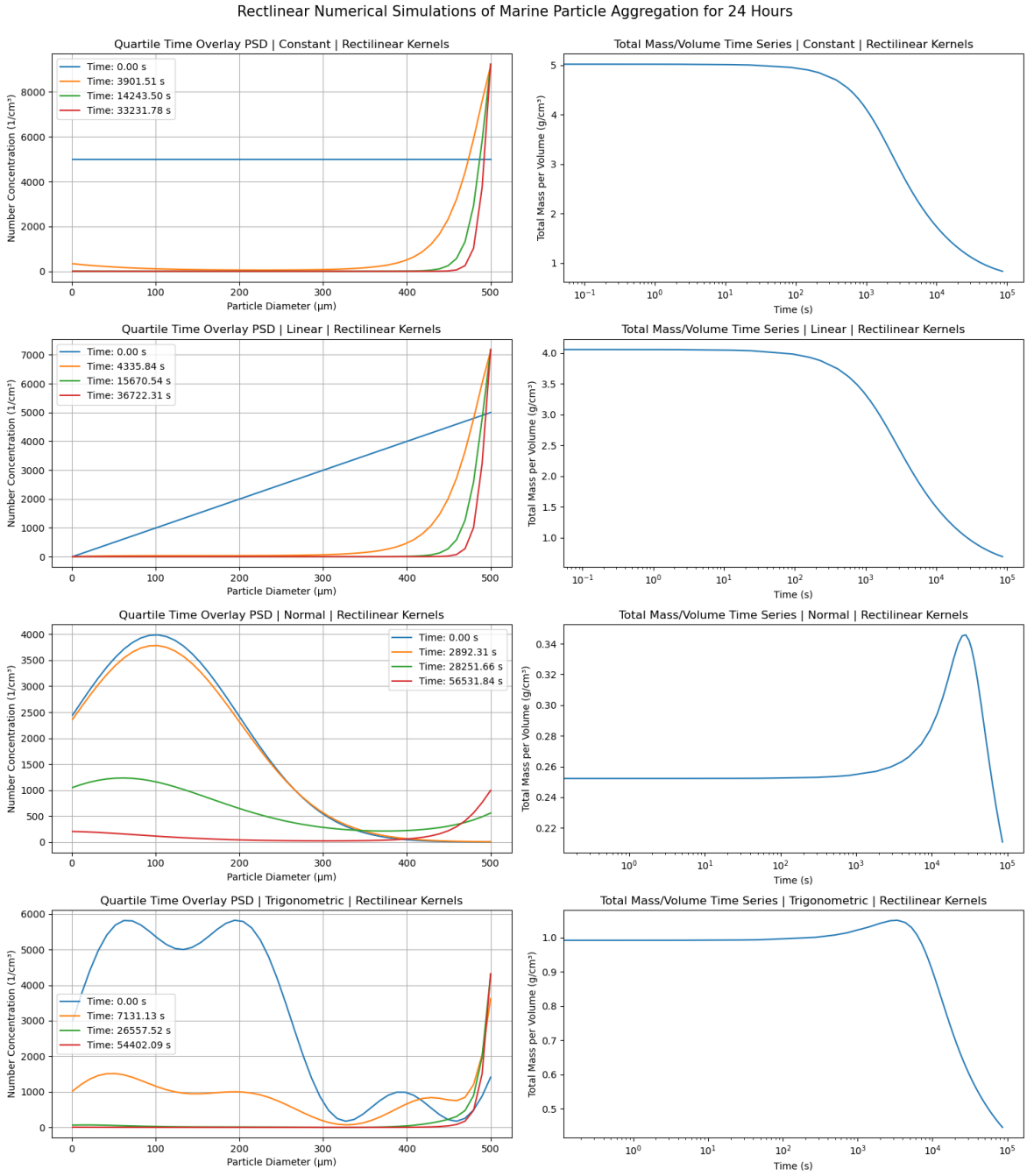

Figure A2. Rectilinear Numerical Simulations of Marine Particle Aggregation for 24 Hours. The figure presents the results of numerical simulations using rectilinear kernels for marine particle aggregation over a 24-hour period. The left column shows the particle size distribution (PSD) over time for different initial conditions: constant, linear, normal, and trigonometric. The right column displays the corresponding total mass per volume time series. Each subplot in the left column illustrates the number concentration of particles across various diameters at specific time intervals, while the subplots in the right column show the evolution of total mass per volume, highlighting the dynamics of mass conservation and aggregation processes.

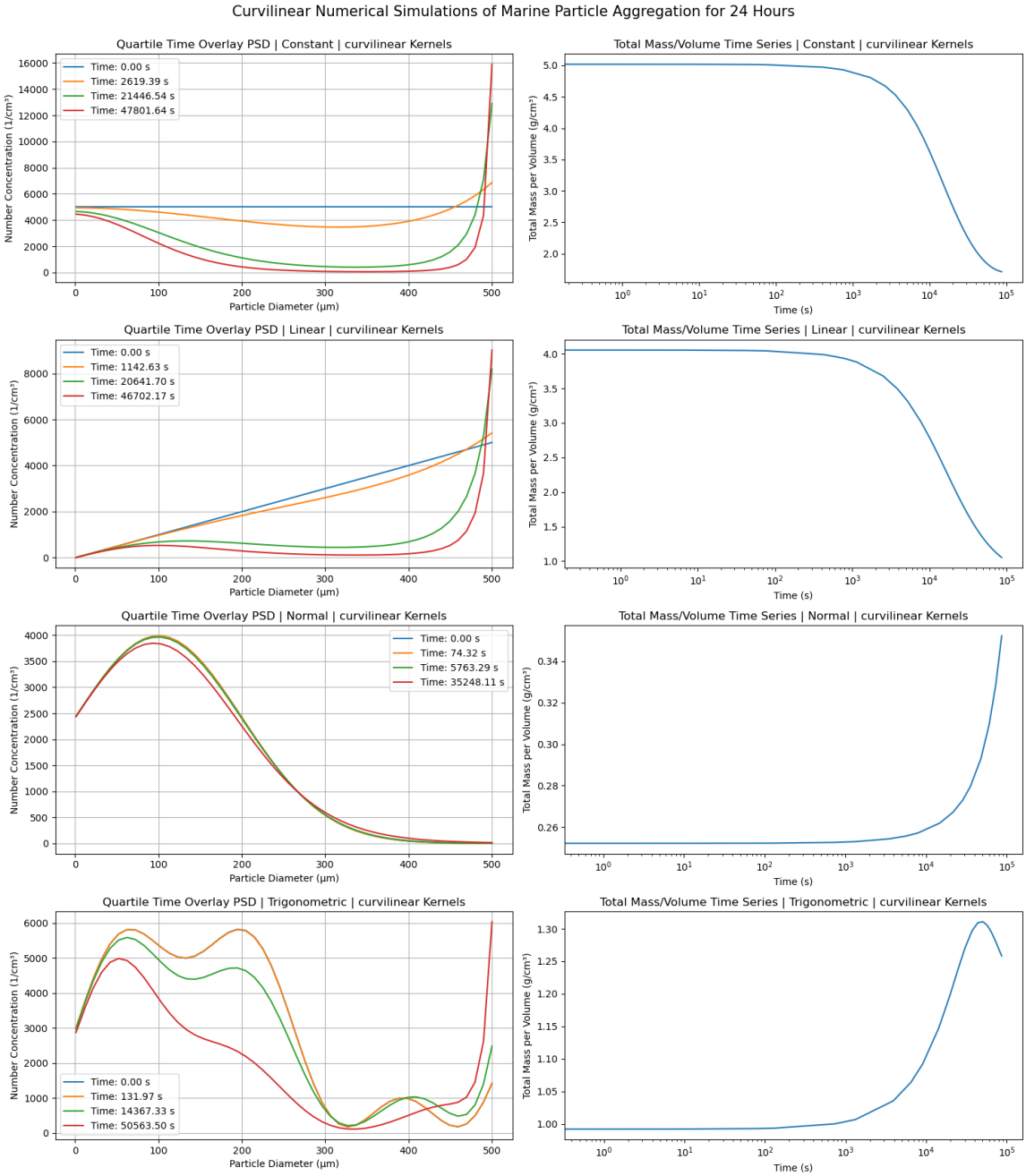

Figure A3. Curvilinear Numerical Simulations of Marine Particle Aggregation for 24 Hours. The figure presents the results of numerical simulations using curvilinear kernels for marine particle aggregation over a 24-hour period. The left column shows the particle size distribution (PSD) over time for different initial conditions: constant, linear, normal, and trigonometric. The right column displays the corresponding total mass per volume time series. Each subplot in the left column illustrates the number concentration of particles across various diameters at specific time intervals, while the subplots in the right column show the evolution of total mass per volume, highlighting the dynamics of mass conservation and aggregation processes under the influence of hydrodynamic effects.